Quantum decay into a continuum at weak bias

Peter Hanggi,* Ulrich Weiss,† and Peter S. Riseborough
Physics Department, Polytechnic University, 333 Jay Street, Brooklyn, New York 11201
(Received 29 January 1986; revised manuscript received 28 July 1986)

We consider the quantum decay from the locally stable ground state of a one-dimensional metastable potential. We consider the case where the metastable minimum is almost degenerate with the vacuum level. In this case, the quantum decay probability is influenced by backscattering from the continuum states; a feature which is not accounted for in standard WKB theory. We evaluate the decay rates, from the ground state and the higher-resonance states, by the use of complex-time path-integral methods. The decay rate from the low-lying states of the metastable well is characterized by two quasi-zero-modes and a transmission factor, which approaches zero proportional to the square root of the potential drop. Moreover, we present a useful set of rules for the complex-time path-integral phase factors. These rules considerably simplify the calculation of decay rates (i.e., the pole condition of the Fourier-transformed Green's function).

I. INTRODUCTION

The problem of escape from a metastable state has long been a subject of theoretical attention. In many situations, the escape is controlled by thermally activated events, for which a classical description is usually adequate.[1] In this paper, our focus will be on a metastable state that has its decay dynamics solely governed by quantum fluctuations, at zero temperature. α-particle decay of nuclei represents an archetype of such a situation. As is well known, the original works of Gamow,[2] Condon and Gurney,[3] and Laue[4] represent milestones in the theory of particle decay. Since then, this problem has been studied extensively.[5] In all the single-particle theories, the tunneling decay probability Γ is decomposed into the form $\Gamma = A\exp(-B)$, i.e., a prefactor A, and an exponential, quantum-mechanical penetration factor B. The exponential $B(E)$ is the "Gamow factor" and is given by

$$\exp[-B(E)] = \exp\left[-2\int_{q_1}^{q_2} dq\{2M[V(q)-E]\}^{1/2}/\hbar\right], \quad (1.1)$$

where M denotes the mass of the tunneling particle, E its energy, and $V(q)$ is the metastable (single-particle) potential field. The expression entering the exponent of (1.1) coincides with the Euclidean action, evaluated along the quasiclassical path $q(\tau)$, at energy $-E$. That is, the action is calculated along the classical path in the inverted potential $-V(q)$ which satisfies

$$M\frac{d^2q}{d\tau^2} = \frac{dV(q)}{dq} \quad (1.2)$$

and has turning points q_1 and q_2 $[\dot{q}_1(0)=\dot{q}_2(\frac{1}{2}T(-E))=0]$. The prefactor is given by

$$A(E) = \frac{\omega_1(E)}{2\pi} = \frac{1}{T(E)}, \quad (1.3)$$

where $T(E)$ is the period of the classical trajectory of energy E, in the metastable well.

The standard result, (1.1), can be obtained through a variety of different techniques. For example, it can be obtained by matching local solutions of the Schrödinger equation onto an outgoing scattering wave function. The matching conditions result in a nonlinear algebraic equation which determines complex values z_n associated with the resonances. The real part of z_n gives the resonance energy E_n and the imaginary part is related to the decay rate Γ_n through

$$\Gamma_n = 2\,\mathrm{Im}z_n/\hbar\,. \quad (1.4)$$

An alternative technique, which is particularly suited to the task of obtaining analytic solutions, is based on Feynman's functional integral formulation of quantum mechanics, as popularized in Ref. 6. This approach is particularly useful since it provides a great deal of physical insight into the multiple-scattering processes which give rise to the formation of the resonances, as well as their decay. Such physical insight is afforded by the description in terms of motion in a potential field, and therefore forms a natural bridge between our classical intuition and quantum mechanics. Furthermore, the path-integral method also allows one to systematically incorporate higher-order effects.

The advantages of the functional integral formulation of quantum mechanics has received wide recognition. There have been many applications in a numerous variety of fields including field theory,[7] particle physics,[8–11] nuclear physics,[12] atomic physics,[13] and chemical physics.[14]

The standard WKB result contained in Eqs. (1.1) and (1.3) may be derived by the path-integral method, by summing over the contributions to the trace of a propagator

$$G(E) = \mathrm{Tr}(\hat{H}-E)^{-1}\,. \quad (1.5)$$

The contributions to the functional integral expression come from paths of fixed energy E which traverse the classically allowed regions of space, and may also enter into the classically forbidden regions. In these latter regions, the momentum takes on imaginary values and since the coordinate is real, one is quite naturally lead to the concept of an imaginary increment of time, and therefore complex times. The WKB result (1.1) has been derived by the complex-time, stationary-phase approximation in

Refs. 9 and 12(a).

Recently, it has been shown[11] that in order to get agreement with the correct physical result, the complex-time functional expression for $G(E)$ has to be evaluated without using the stationary-phase approximation.

In this work, we consider the quantum decay of a particle of mass M moving in a one-dimensional metastable potential well described by $V(q)$. The type of potential $V(q)$ is sketched in Fig. 1. In the situation under consideration, the energy of the metastable ground state may only slightly exceed the vacuum level of the continuum. As we shall see later, the calculation of the decay rate from low-lying levels of the metastable well is considerably more complicated than the corresponding calculations of quantum decay from other metastable potentials, such as the cubic potential.

The calculation of the rate requires one to find the paths which traverse the classically forbidden regime and maximize the action. Such trajectories which traverse the classically forbidden region once are often referred to as "instantons" or "kinks," and the time-reversed paths as "anti-instantons" or "antikinks." An instanton—anti-instanton pair is often called a "bounce" trajectory.

The decay rate is predominantly governed by the bounce trajectory $q_B(\tau)$, which is a stationary point of the action in the classically forbidden region. This bounce trajectory, however, is not uniquely defined since a time translation $q_B(\tau)\rightarrow q_B(\tau+\tau_0)$ also satisfies the same boundary conditions and yet leaves the action invariant. This time-translational symmetry is revealed by an exact fluctuation eigenmode proportional to $\dot{q}_B(\tau)$ with zero eigenvalue. This fluctuation eigenmode restores the time translational invariance of the system, when a specific bounce trajectory is being considered. When one considers the decay of low-lying states, there are additional complications that one should take into account, that are not included in the standard WKB. First, the time separating the instanton—anti-instanton pair which forms the bounce becomes quite large when compared to the time that is required for the instanton trajectory to cross the classically forbidden region. This large bounce time generates another approximate invariance of the system, namely the approximate invariance obtained by varying the time separation between the instanton and anti-instanton trajectory. This approximate invariance manifests itself in a quasi-zero-mode, the breathing mode, which describes the relative motion between the instanton and anti-instanton solutions. This quasi-zero-mode requires careful consideration. The second complication occurs due to the strong influence that backscattering from the continuum has on the decay rate. The complex-time path-integral formalism[7–12] provides an appropriate vehicle for deriving analytic expressions in this situation. Here, we shall extend previous results by one of the authors.[11]

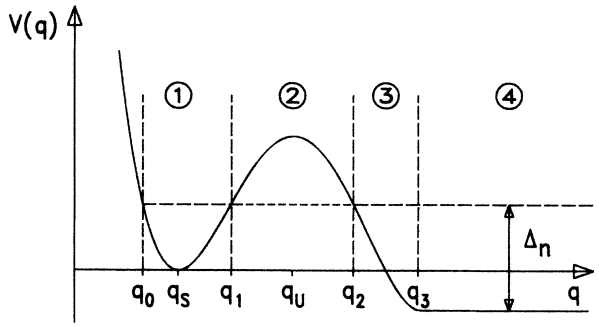

FIG. 1. A schematic diagram of a potential having metastable states, and having a small potential drop between the metastable minimum and the vacuum level of the continuum. The drop between the energy of the nth metastable state E_n and the lowest level of the continuum is denoted by Δ_n. The intercepts q_0, q_1, and q_2 are the turning points of classical motion in regions 1 and 3, respectively. The frequency of small oscillations within the metastable well is denoted by ω_1. We consider a specific potential in which $V(q)=-\hbar\omega_3\delta$ for $q>q_3$ where δ is a constant. The curvature of the potential has a discontinuity at q_3, of magnitude $V''(q_3-\epsilon)-V''(q_3+\epsilon)=M\omega_3^2$.

The study of this particular type of decay problem possesses interesting applications in nuclear, or particle physics[8–12] or in the dynamics of superconducting devices.[15] As examples, there is the problem of α-particle decay in nuclei, with a resonance state that lies close to the continuum level, and we also mention the quantum decay of macroscopic metastable states that occurs in current-biased Josephson junctions or superconducting quantum interference devices.[16] In these latter devices, the junctions can be manufactured with parameters such that the effect of dissipation is weak, and that the metastable states are energetically close to the continuum level.

II. QUANTUM DECAY FROM LOW-LYING STATES

The standard WKB path-integral methods[6–8,12(a)] are not directly applicable to the calculation of the decay rate from the potential form sketched in Fig. 1. In what follows, we will employ the complex-time path-integral language, developed in Refs. 7–14.

We consider the trace of the Fourier-transformed propagator, $G(E)$,

$$G(E)=\mathrm{Tr}\left[\frac{1}{\hat{H}-E}\right]=\frac{i}{\hbar}\int_0^\infty dt\,\exp(iEt/\hbar)\times\int dq\langle q\mid\exp(-i\hat{H}t/\hbar)\mid q\rangle\ . \quad (2.1)$$

The time-dependent propagator in (2.1) can be directly expressed in terms of a Feynman path integral over closed paths ($q_i=q_f$); i.e.,

$$K(q_f,t;q_i,0)=\langle q_f\mid\exp(-i\hat{H}t/\hbar)\mid q_i\rangle=\int_{q_i}^{q_f}\mathscr{D}q(t)\exp[iS(q(t))/\hbar]\ . \quad (2.2)$$

Here, S denotes the action, evaluated along the path $q(t)$; i.e.,

$$S=\int_0^t[\tfrac{1}{2}M\dot{q}(s)^2-V(q(s))]ds\ . \quad (2.3)$$

In order that (2.1) be defined properly, the time t must be assigned a very small negative imaginary part γ.[11,13] The diagonal form of the (closed-path) propagator leads to

four distinct contributions to $G(E)$;

$$G(E)=\sum_{i=1}^{4} G_i(E) . \tag{2.4}$$

The G_i are determined by the trajectories which begin and end in region i, as depicted in Fig. 1. We note that in order to have periodic paths in region 4, it is convenient to truncate the potential at $q=L$ with an infinite barrier for $q \geq L$, and then take the limit of L going to infinity.

Due to the Hermiticity of the single-particle Hamiltonian, $G(E)$ only possesses poles on the real E axis. Thus, the decay rates cannot be found directly. However, if one continues the energy E to a value slightly above the real axis in the complex E plane,[11,12] then one can find the decay rates for the metastable states of potentials of the type depicted in Fig. 1. This continuation has the effect of exponentially suppressing the contributions to $G(E)$ from the paths in region 4. The paths in region 4 have a factor of $\exp(-\gamma\pi/\zeta)$ associated with them, where ζ is the level spacing of the quasicontinuum in region 4. Hence, in the limit $L\to\infty$, $\zeta\to 0$, and the contributions from region 4 are entirely negligible. The assumption that γ is much smaller than the rate which we desire means that the imaginary part of E is still negligible in regions 1 and 2. Furthermore, the contribution of G_2 to (2.4) is also exponentially suppressed by a barrier penetration factor, when compared to G_1. Therefore, the dominant contribution to the decaying states comes from G_1, i.e.,

$$G(E)\simeq G_1(E) . \tag{2.5}$$

The quantity in (2.5) does include contributions from paths which make excursions into regions 2 and 3 but neglects those which enter region 4. The closed-path propagator $G_1(E)$ exhibits poles at the (complex-valued) resonance energies

$$z_n=E_n-i\hbar\Gamma_n/2 , \tag{2.6}$$

where Γ_n is the decay rate of the metastable state with energy E_n. The contributions of the various paths are calculated in the manner outlined in Ref. 11. First, if we restrict the closed paths to remain entirely within the classically allowed region $i=1$ (a Minkowskian region), one obtains a contribution to G_1 of

$$G_1^{(1)}(E)=\frac{i}{\hbar}T(E)\frac{U_1(E)}{1-U_1(E)} \tag{2.7}$$

from a summation over all the multiple cycles within region 1. In (2.7), $T(E)$ is the period of the closed classical path of energy E, in region 1, and

$$U_1(E)=-\exp[iW_1(E)/\hbar] \tag{2.8a}$$

denotes the contribution from one cycle with two "reflections" at each of the classical turning points, and

$$W_1(E)=2\int_{q_0}^{q_1}\{2M[E-V(q)]\}^{1/2}dq . \tag{2.8b}$$

The classical turning points q_0 and q_1 are found from the energy

$$E=\tfrac{1}{2}M\dot{q}^2+V(q) \tag{2.9}$$

from the condition $\dot{q}=0$. As is evident from the form of (2.7), the multiple cycles lead to a geometric series. The contribution $G_1^{(1)}(E)$ given by (2.7) only exhibits poles on the real axis, with unit residues. The poles are located at the energies

$$E_n^{(1)}=\hbar\omega_1(n+\tfrac{1}{2}),\quad \omega_1^2=\frac{1}{M}V''(q_s)$$

which represents the approximate harmonic nature of the metastable well. At these energies, we have $W_1(E_n^{(1)})=(n+\frac{1}{2})2\pi\hbar$.

In order to obtain decay rates Γ_n, we clearly must also account for the global structure of the potential field $V(q)$. Thus, we must include contributions to $G_1(E)$ which stem from paths which enter into regions 2 and 3. Therefore, we must, for example, also take into account those paths which start at a point q_i inside region 1, then enter into the classically forbidden region (2) at q_1. These paths are either "reflected" at point q_2, or are continued into region 3. The paths that enter region 3 are reflected backwards at point q_3, where $V''(q)$ is discontinuous. All these paths eventually return to their starting point q_i, via a detour which passes through the turning point at q_0.

Inside the classically forbidden region, $z<V(q)$, we must consider the imaginary time trajectories;[6-8] i.e.,

$$M\frac{d^2q_c}{d\tau^2}=\frac{dV(q_c)}{dq_c} , \tag{2.10}$$

which describes classical motion in the inverted potential. In this, τ is a Euclidean time obtained through a formal analytic continuation $\tau=it$ of the Minkowskian time t. The corresponding Euclidean action is defined as $(-i)$ times the analytic continuation of the Minkowskian action. The action associated with one traversal of the barrier region is given by

$$S=B(z)+\tau z , \tag{2.11a}$$

$$B(z)=\int_{q_1}^{q_2}\{2M[V(q)-z]\}^{1/2}dq . \tag{2.11b}$$

Next, we focus attention on the low-lying metastable states, for which $z=O(\hbar\omega_1)$. In the case of a small potential drop, $\hbar\omega_3\delta=O(\hbar\omega_1)$, the path which enters the Eu-

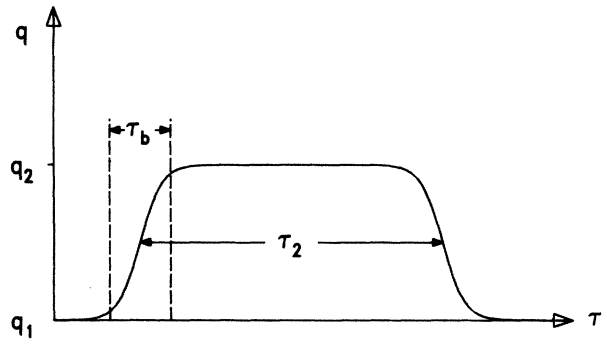

FIG. 2. The trajectory of an extended bounce (a kink-antikink configuration) which extends between the turning points q_1 and q_2. In this, τ_b is the kink width while τ_2 is the length of the bounce.

clidean region will remain close to the classical turning points q_1 and q_2 for long periods of time, but will move rapidly through the valley of the inverted potential $\hat{V}(q)=-V(q)$, see (2.10). The form of this instanton–anti-instanton trajectory is sketched in Fig. 2. The trajectory is characterized by two time scales: the time τ_b, required to traverse the valley region of $\hat{V}(q)$, $\tau_b \simeq 1/\omega_u$, where $\omega_u^2 = |V''(q_u)|/M$, and the "length" or the long time $\tau_2(\delta)$ that the path resides near the turning point q_2. Each traversal of the Euclidean region ($i=2$), is a kinklike trajectory for which the action has an approximate time-translational symmetry. This very feature clearly plagues the evaluation of the Fourier-transformed propagator in (2.1). To deal with the quasi-zero-mode problem we introduce an improved semiclassical kernel $\bar{K}_s(q_f,t;q_i)$ as a convolution of standard semiclassical kernels K_s (Ref. 11),

$$\bar{K}_s(q_f,t;q_i)=\int_0^t dt_1 K_s(q_f,t-t_1;q_m)\dot{q}_c(t_1) \times K_s(q_m,t_1;q_i)\ , \tag{2.12a}$$

where q_m is an intermediate point between q_i and q_f. The semiclassical kernel, K_s, follows from (2.2) by use of the stationary-phase approximation as

$$K_s(q',t;q)=\left[\frac{i}{2\pi\hbar}\right]^{1/2}\left[\dot{q}_c(0)\dot{q}_c(t)\frac{\partial^2 W}{\partial E^2}\right]^{-1/2} \times \exp[iS(q_c(t))/\hbar]\ . \tag{2.12b}$$

Here $q_c(s)$ is the classical path with boundary conditions, $q_c(0)=q$ and $q_c(t)=q'$.

First consider the case where the path from q_i to q_f lacks the quasi-zero-mode problem. Then, the remaining t_1 integral in (2.12a) may be evaluated in the stationary-phase approximation. This yields $\bar{K}_s(q_f,t;q_i)=K_s(q_f,t;q_i)$, where K_s is explicitly given by Eq. (2.12b). Next, suppose that the potential is such that the classical path from q_i to q_f is a kinklike trajectory. Then, by choosing $q_m=q(t_1)$ as the center of the kink, the t_1 integral in (2.12a) takes into account the displacement of the kink, which arises from the large fluctuation associated with the quasi-time-translation invariance of the kink action. Since the action terms entering (2.12a) depend for large (but finite) t only weakly on t_1, the stationary-phase approximation of the time integral in (2.12a) is no longer applicable.

On summary, the merit of the expression (2.12a) is that all fluctuations which influence the shape of the kink are dealt with within the Gaussian approximation only, while the large fluctuation mode, leading to a displacement of the kink, is taken into account exactly.

Now consider a closed cycle which starts at q_i, where q_i is in region 1 (see Fig. 1), then crosses the barrier at q_u, is reflected at q_3, then penetrates the barrier again at q_2 in the reverse direction, and returns to the starting point q_i, via a detour to the turning point at q_0 (see Fig. 1). This path contains a complete cycle in the barrier region (Euclidean time), which consists of a kink-antikink pair (see Fig. 2). Hence, two quasi-zero-eigenvalues are involved in the spectrum of fluctuation modes. These quasi-zero-modes are associated with the displacement of the two kink centers. Clearly, the improved semiclassical kernel for this path is written as a convolution of three semiclassical kernels; i.e.,

$$\bar{K}_s(q_i,t;q_i,0)=-[2V(q_u)/M]\int_0^t dt_1\int_0^{t_1} dt_2 K_s(q_i,t-t_1;q_0;q_u)K_s(q_u,t_1-t_2;q_2;q_3;q_u)K_s(q_u,t_2;q_i)\ . \tag{2.13}$$

The velocity has been evaluated at $q=q_u$. The points q_0,q_u,q_3 are depicted in Fig. 1. The additional parameters $\{q_0,q_2,q_3\}$ in the propagators are merely to remind us of the turning points and the reflection at q_3. Moreover, it should be noted that the path which executes the above cycle in the reverse direction must be omitted, in order to avoid double counting. This time-reversed path yields an expression that is identical to (2.13). The above equation is then transformed to Euclidean time $\tau=it$, and the convolutions inherent in (2.13) are evaluated in the same way as in Ref. 11, Eqs. (2.20)–(2.27). In doing so, one accounts for multiple cycles in the region $i=2$ and 3. All these various contributions lead to geometric series, just as in the case in (2.7). Care must be taken to include the appropriate phase factors at the classical turning points, as well as the reflection coefficient at q_3. These factors are discussed extensively in the Appendix. The result of this exercise is given by

$$G(z)\simeq G_1(z)=\frac{i}{\hbar}\frac{T(z)U_1(z)[1+ir_3F_3(z)]}{[1-U_1(z)][1+ir_3F_3(z)]+\frac{1}{4}[1+U_1(z)]Y_2(z)\tilde{Y}_2(z)[1-ir_3F_3(z)]}\ . \tag{2.14}$$

Here, $U_1(z)$ is given by (2.8a), r_3 is the reflection coefficient at q_3 and $F_3(z)$,

$$F_3(z)=\exp[iW_3(z)/\hbar]\ , \tag{2.15}$$

is the phase associated with a cycle in the Minkowskian region $i=3$. The factors Y_2 and $\tilde{Y}_2$ are the contributions of the two half cycles in region 2 that both start and end at q_u, but return via a reflection at the turning points q_1 and q_2, respectively. These factors are given by the explicit expressions

$$Y_2(z)=[2V(q_u)/M]^{1/2}\int_\alpha dt\exp(izt/\hbar)K_s(q_u,t;q_1;q_u)\ , \tag{2.16}$$

$$\tilde{Y}_2(z)=[2V(q_u)/M]^{1/2}\int_\alpha dt\exp(izt/\hbar)K_s(q_u,t;q_2;q_u)\ ,$$

where α is the integration contour in the complex t plane

which passes through all the stationary points of the integrand. The pole condition of (2.14), will be rederived by an alternative method in the Appendix. The position of the poles, z_n, can be evaluated iteratively. Using the harmonic energies $E_n=\hbar\omega_1(n+\frac{1}{2})$, and on observing that

$$1-U_1(z_n)=1+\exp\left[\frac{i}{\hbar}(2\pi z_n/\omega_1)\right] \simeq -\frac{\pi}{\omega_1}\Gamma_n \tag{2.17}$$

from (2.6), one can then obtain the expression for the decay rate $\Gamma(E_n)=\Gamma_n$,

$$\Gamma_n=\frac{\omega_1}{2\pi}Y_2(E_n)\tilde{Y}_2(E_n)\,\mathrm{Re}\left[\frac{1-ir_3F_3(E_n)}{1+ir_3F_3(E_n)}\right], \tag{2.18}$$

wherein Re stands for the real part. For the low-lying states, where $E_n=O(\hbar\omega_1)$, the integration in (2.16) can no longer be performed within the steepest-descent approximation. This reflects the fact that a considerable contribution to the integrals come from energy values at which the assumption of the smoothness of $\partial^2W/\partial E^2$ no longer applies. Therefore, we must go beyond the usual approximation for the Euclidean factor $Y_2(E_n)$. Following Ref. 11 Eqs. (2.33)–(2.35), the explicit result for $Y_2(E_n)$ is expressed in terms of a parameter A_0 that describes the asymptotic behavior of the instanton trajectory $\bar{q}_0(\tau)$, near q_s, with energy $E=0$,

$$\bar{q}_0(\tau)\underset{\tau\to-\infty}{\to}q_s+\frac{A_0}{2M\omega_1}\exp(+\omega_1\tau), \tag{2.19}$$

where $\bar{q}_0(0)=q_u$. Correspondingly, $\tilde{Y}_2(E_n)$ is expressed in terms of the parameter A_δ characterizing the instanton path $\bar{q}_\delta(\tau)$, near q_3, with energy $E=-\hbar\omega_3\delta$,

$$\bar{q}_\delta(\tau)\underset{\tau\to+\infty}{\to}q_3-\frac{A_\delta}{2M\omega_3}\exp(-\omega_3\tau), \tag{2.20}$$

where $\bar{q}_\delta(0)=q_u$. The constants A_0 and A_δ depend on the explicit details of the barrier shape. The contributions from the two half cycles in region 2 are then given by[11]

$$Y_2(E_n)=\frac{(2\pi)^{1/2}}{\Gamma(n+1)}\left[\frac{A_0^2}{2M\hbar\omega_1}\right]^{n+1/2}\times\exp[-S_1(\bar{q}_0(\tau))/\hbar] \tag{2.21}$$

and

$$\tilde{Y}_2(E_n)=\frac{(2\pi)^{1/2}}{\Gamma(\nu+1)}\left[\frac{A_\delta^2}{2M\hbar\omega_3}\right]^{\nu+1/2}\exp[-S_2(\bar{q}_\delta(\tau))/\hbar]. \tag{2.22}$$

In this expression, we have made use of the notation

$$\Delta_n-E_n=\hbar\omega_3\delta=\hbar\omega_3(\nu+\tfrac{1}{2})-\hbar\omega_1(n+\tfrac{1}{2}),$$

i.e.,

$$\nu=\left[\frac{\omega_1}{\omega_3}\right](n+\tfrac{1}{2})-\tfrac{1}{2}+\delta. \tag{2.23}$$

The total bounce action S is given by

$$S=S_1+S_2, \tag{2.24}$$

where S_1 is the contribution from the left half cycle; i.e.,

$$S_1(\bar{q}_0(\tau))=2\int_{q_s}^{q_u}dq[2MV(q)]^{1/2}, \tag{2.25a}$$

and S_2 is the contribution from the right half cycle with energy $E=-\hbar\omega_3\delta$; i.e.,

$$S_2(\bar{q}_\delta(\tau))=2\int_{q_s}^{q_u}dq\{2M[V(q)+\hbar\omega_3\delta]\}^{1/2}. \tag{2.25b}$$

On combining (2.21)–(2.25) with (2.18), and using both the expressions for $F_3(E_n)$,

$$F_3(E_n)=\exp[i\pi(\nu+\tfrac{1}{2})]=i\exp(i\pi\nu), \tag{2.26}$$

and the transmission coefficient $\mathcal{T}(\nu)$,

$$\mathcal{T}(\nu)=\mathrm{Re}\left[\frac{1+r_3\exp(i\pi\nu)}{1-r_3\exp(i\pi\nu)}\right], \tag{2.27}$$

one can obtain the quantum decay rate Γ_n. This yields the main result of this paper,

$$\Gamma_n=\omega_1\frac{1}{\Gamma(n+1)\Gamma(\nu+1)}\left[\frac{A_0^2}{2M\hbar\omega_1}\right]^{n+1/2}\times\left[\frac{A_\delta^2}{2M\hbar\omega_3}\right]^{\nu+1/2}\mathcal{T}(\nu)\exp(-S/\hbar). \tag{2.28}$$

The reflection coefficient r_3, is determined by smoothly matching a plane wave in the region $i=4$ onto a Weber parabolic cylinder function[17] in the region $i=3$ [see the Appendix, Eq. (A8)]. This yields the explicit result

$$r_3=\frac{\kappa_\nu-1}{\kappa_\nu+1}, \tag{2.29}$$

where

$$\kappa_\nu=\left[\frac{2}{\nu+\frac{1}{2}}\right]^{1/2}\frac{\Gamma(1+\nu/2)}{\Gamma(\frac{1}{2}+\nu/2)}. \tag{2.30}$$

The transmission coefficient is then evaluated as

$$\mathcal{T}(\nu)=\left[\frac{1}{\kappa_\nu}\cos^2\left[\frac{\nu\pi}{2}\right]+\kappa_\nu\sin^2\left[\frac{\nu\pi}{2}\right]\right]^{-1}. \tag{2.31}$$

We shall now examine the limiting behavior exhibited by the result (2.28) and (2.31).

When the energy of the nth metastable state E_n becomes degenerate with the vacuum level, i.e., $\Delta_n\equiv\hbar\omega_3(\nu+\frac{1}{2})\to0$, then from (2.31) one finds that

$$\mathcal{T}(\nu)\underset{\Delta_n\to0}{\to}\sqrt{2}\frac{\Gamma(\frac{1}{4})}{\Gamma(\frac{3}{4})}\left[\frac{\Delta_n}{\hbar\omega_3}\right]^{1/2} \simeq 4.18(\nu+\tfrac{1}{2})^{1/2}. \tag{2.32}$$

Hence, as the potential drop between the energy level and the vacuum level vanishes, the decay rate Γ_n approaches zero proportional to the square root of the potential drop Δ_n. The standard WKB result (1.1) and (1.3), by contrast, completely fails to predict this behavior, since it does not involve any details of the potential in regions 3 and 4.

TABLE I. The transmission factor $\mathcal{T}(\nu)$, (2.31), for $\omega_1=\omega_3$, as a function of the quantum number n of the metastable state for different biases δ, (2.23). For a large bias ($\delta \gg 0$) the transmission factor approaches unity.

	$\delta=-0.5$	$\delta=-0.45$	$\delta=-0.25$	$\delta=0$	$\delta=0.25$
$n=0$	0	0.8182	1.1808	1.1283	1.0490
$n=1$	0.9990	0.9927	0.9778	0.9772	0.9875
$n=2$	0.9999	1.0020	1.0079	1.0093	1.0055
$n=3$	1.0000	0.9990	0.9960	0.9952	0.9970

When the potential drop is large, $\nu \gg 1$, the Γ function in (2.30) may be approximated by the Stirling formula. The transmission coefficient $\mathcal{T}(\nu)$ rapidly approaches unity, and (2.28) reduces to

$$\Gamma_n=\frac{\omega_1}{\Gamma(n+1)}\left[\frac{A_0^2}{2M\hbar\omega_1}\right]^{n+1/2}\exp(-\tilde{S}/\hbar)\,, \quad (2.33)$$

where $\tilde{S}$ is given by

$$\tilde{S}=S-\frac{\Delta_n}{2\omega_3}\left[1+\ln\left[\frac{A_\delta^2}{2M\omega_n}\right]\right] \quad (2.34)$$

and corresponds to the action of one cycle in the Euclidean region with energy $E=0$ [also see Eq. (A8) in Ref. 11]. Since the breathing mode of the bounce is no longer a quasi-zero mode, when the potential drop Δ_n is large, the limit result (2.33) is identical with that obtained by the standard bounce method.[7(b)]

If one examines the rate of decay from the metastable states with high energies E_n, one can reduce the general expression into the standard WKB result. At high energies E_n, $n \gg 1$ (but E_n still not of the order of the barrier height V_b), the remaining n dependence in (2.33) can be simplified with the aid of Stirling's approximation. If one assumes that the turning points q_1 and q_2 are still near the harmonic region of the potential well, then the penetration factor (1.1) can be obtained from (2.33) as

$$B(E)=\tilde{S}-\frac{E}{2\omega_1}\left[1+\ln\left[\frac{A_0^2}{2ME}\right]\right]\,, \quad (2.35)$$

where $\tilde{S}$ is given in (2.34). Hence, in the limit $\nu \gg 1$ and $n \gg 1$ we recover the standard WKB rate

$$\Gamma(E)=\frac{\omega_1}{2\pi}\exp[-B(E)/\hbar]\,. \quad (2.36)$$

The deviation of the full expression (2.28) for the rate, from the standard WKB result may be surmised from examining Table I, which shows the values of $\mathcal{T}(\nu)$ for the various resonant levels, denoted by n, for five different values of the bias δ. We have chosen the value of ω_1/ω_3 equal to unity. We note that $\mathcal{T}(\nu)$ approaches 0 for the $n=0$ resonance, when $\delta=-\frac{1}{2}$; i.e., the ground state matches with the continuum level. In this case, the transmission factors for all the other resonance levels are close to unity. Thus WKB is extremely good for all the levels except the $n=0$ level. As the bias increases, the value of $\mathcal{T}(\nu)$ rapidly increases for the $n=0$ level, but one notes that the $\mathcal{T}(\nu)$ starts to oscillate as n is varied.

The other factors involved in the deviation from the standard WKB result is the presence of the Γ functions in the place of Stirling's approximation. The effect of these factors are not as dramatic, *they merely give rise to a small* diminuition of the rate from its WKB value.

III. DISCUSSION AND CONCLUSION

We have evaluated the quantum decay rate for a particle to tunnel out of a metastable state, into a semi-infinite well in which the potential is bounded from below. There exists a threshold for tunneling decay to occur; this simply corresponds to the matching of the energy of the metastable state with the lowest energy level of the continuum. We have investigated the decay rates, paying particular attention to the behavior near this threshold. The decay rate is found from the poles of a Green's function $G(E)$. The Green's function is expressed as a Laplace transform of a Feynman path integral. The effect of tunneling and backscattering from the final continuum states are accounted for by summing up contributions from paths, in complex time, that traverse both the classically allowed and the classically forbidden regions. In order to obtain the correct form of the rate in the vicinity of the threshold, it was necessary to evaluate certain crucial contributions, (2.21) and (2.22), by going beyond the stationary-phase approximation. The prefactor of the resulting rate involves a transmission factor $\mathcal{T}(E)$. The transmission factor approaches unity for the highly excited states, and the rate reduces to previously derived expressions. As the threshold is approached, the rate vanishes in proportion to the square root of the energy difference between the metastable ground state and the lowest level of the continuum.

ACKNOWLEDGMENTS

This work has been supported in part by the Office of Naval Research under Contract No. N00014-85-K-0372 and the U. S. Department of Energy, under Grant No. DE-FG02-84-ER45127, and also by the Deutsche Forschungsgemeinschaft.

APPENDIX

In this appendix, we present a prescription for evaluating contributions to the complex-time path integrals that prove to be extremely useful in obtaining the pole conditions of the type used in Eq. (2.14). As is well known,[18] the phase of a semiclassical amplitude is influenced by the

number of turning points along a particular trajectory. In complex-time trajectories, the phase of the semiclassical amplitude is determined not only by the trajectories which undergo multiple reflections in Minkowskian regions of phase space, but also undergo multiple reflections in Euclidean regions and transmissions between the Minkowskian and Euclidean regions, or vice versa. We introduce the following notation: r_M is the reflection coefficient for the amplitude at a classical turning point in a Minkowskian (real time) region, r_E is the reflection coefficient for the amplitude at a classical turning point in an Euclidean (imaginary time) region, t_M is the transmission coefficient for the amplitude for an entry from a Minkowskian region into a Euclidean region, and t_E is the transmission coefficient for the amplitude for an entry from a Euclidean region into a Minkowskian region.

For a smooth potential at the boundary between the Minkowskian and Euclidean region (such as in the harmonic potential) as shown in Fig. 3, one finds on comparing with the results from standard quantum mechanics that

$$r_M=\exp(-i\pi/2),\quad t_M=\exp(-i\pi/2)\ ,\qquad r_E=\tfrac{1}{2}\exp(i\pi/2),\quad t_E=\exp(i\pi/2)\ . \tag{A1}$$

In particular, we note that $r_M^2=\exp(-i\pi)=-1$, which gives the familiar phase for the semiclassical (Minkowskian) amplitude for a path with two turning points, since each turning point contributes a factor of $\exp(-i\pi/2)$ (Refs. 10 and 18) [also note the minus sign in (2.8a)].

We shall now reconsider the pole condition of Eq. (2.14). We denote by $Q=Y_2 u\tilde{Y}_2\hat{u}$ the contribution of one cycle in the Euclidean region ($i=2$), in which Y_2 and $\tilde{Y}_2$ are the contributions of the two half cycles, evaluated in (2.21) and (2.22). The additional factors of u and $\hat{u}$ take into account both the reflections at the turning points q_1 and q_2, respectively, as well as the excursions that penetrate into regions 1 and 3, respectively. The summation over all the multiple cycles in region 2 yields a geometric series

$$\sum_{n=1}^{\infty} Q^n=\frac{Q}{1-Q}\ . \tag{A2}$$

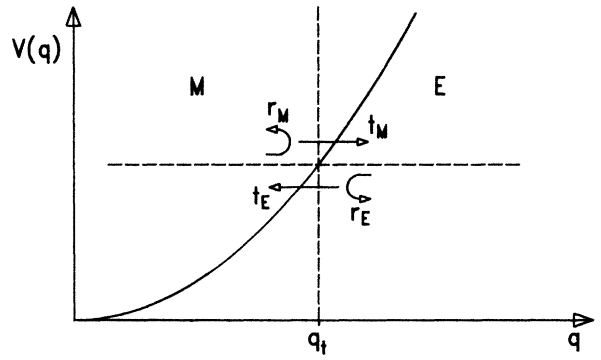

FIG. 3. The coefficients of reflection r and transmission t, that occur at a classical turning point q_t. The indices M and E denote the Minkowskian and Euclidean regions, respectively.

Then one finds the pole condition, $1-Q=0$. Furthermore, since the factor u ($\hat{u}$) is a superposition of a reflection coefficient r_E and a transmission coefficient t_E arising from the boundary between regions 2 and 1 (3). The transmission coefficient is multiplied by a factor representing the sum over any number of cycles in region 1 (3). We denote the contribution arising from one cycle in the Minkowskian region j ($j=1,3$) by

$$F_j(z)=\exp[iW_j(z)/\hbar]\ , \tag{A3}$$

where $W_1(z)$ is defined in (2.8b) and $W_3(z)$ is defined in a similar manner. On attaching the appropriate reflection and transmission factors in the jth Minkowskian region, the pole condition assumes the form

$$1-Y_2\left[r_E+t_E\frac{r_M F_1}{1-r_M r_M F_1}t_M\right]\times\tilde{Y}_2\left[r_E+t_E\frac{r_3 F_3}{1-r_M r_3 F_3}t_M\right]=0\ . \tag{A4}$$

In this expression, r_3 is the reflection factor at $q=q_3$, which arises from the discontinuity of $V''(q)$. If we insert the explicit forms in (A1), the pole condition can be recast as

$$1+Y_2\tilde{Y}_2\left[\frac{1}{2}-\frac{F_1}{(1+F_1)}\right]\left[\frac{1}{2}+\frac{(-i)r_3F_3}{(1+ir_3F_3)}\right]=0$$

or

$$(1+F_1)(1+ir_3F_3)+\tfrac{1}{4}Y_2\tilde{Y}_2(1-F_1)(1-ir_3F_3)=0\ . \tag{A5}$$

If one then puts $F_1=-U_1$, (2.8a), then (A5) becomes identical with the pole condition given in (2.14).

As a second example, we shall consider the double-well potential sketched in Fig. 4. Using similar reasoning, we immediately arrive at the pole condition

$$1-Y_2\left[r_E+t_E\frac{r_M F_1}{(1-r_M r_M F_1)}t_M\right]\times\tilde{Y}_2\left[r_E+t_E\frac{r_M F_3}{(1-r_M r_M F_3)}t_M\right]=0$$

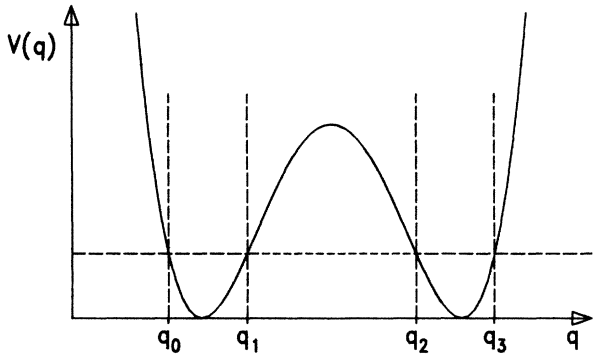

FIG. 4. The classical turning points q_0, q_1, q_2, and q_3 that occur in a double-well potential.

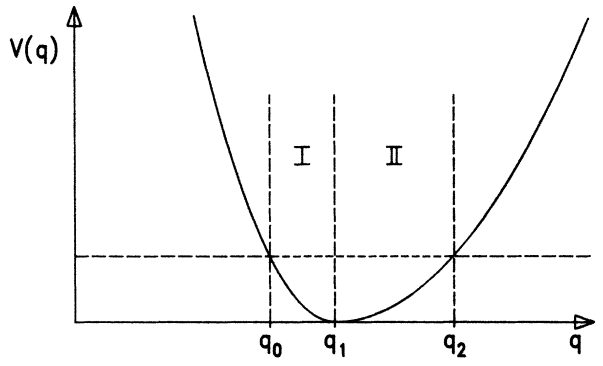

FIG. 5. A potential composed of two semiharmonic wells, of different curvature, connected at $q=q_1$. The turning points of the classical motion are at q_0 and q_2.

which, with $U_1=-F_1$ and $U_3=-F_3$, simplifies to

$$(1-U_1)(1-U_3)+\tfrac{1}{4}Y_2\tilde{Y}_2(1+U_1)(1+U_3)=0\ . \tag{A6}$$

When evaluated within the semiclassical approximation, the pole condition given in (A6) coincides with the pole condition found in Ref. 11, Eq. (2.28), i.e.,

$$(1-U_1)(1-U_3)+Y_2\tilde{Y}_2=0\ . \tag{A7}$$

We shall now evaluate the reflection and transmission coefficients that occur at discontinuities of the potential. By smoothly matching the wave functions across the discontinuity, one finds the expressions for the reflection and transmission coefficients

$$\begin{aligned} r_{\rm I}&=-r_{\rm II}=\frac{k_{\rm I}-k_{\rm II}}{k_{\rm I}+k_{\rm II}}\ , \\ t_{\rm I}&=t_{\rm II}=(1-r_{\rm I}^2)^{1/2}\ , \end{aligned} \tag{A8}$$

where the index I (II) refers to the left-hand (right-hand) side of the boundary. If the potential is discontinuous at $q=q_0$, i.e., $V(q_0-\epsilon)=v_{\rm I}$, $V(q_0+\epsilon)=v_{\rm II}$ and if $V'(q_0-\epsilon)=V'(q_0+\epsilon)=0$, then we find that

$$k_j=[2M(E-v_j)]^{1/2},\quad j={\rm I,II}\ .$$

If the discontinuity only occurs in the curvature of $V(q)$, as is the case at $q=q_3$ in Fig. 1, we find that

$$k_{\rm II}=(2M\Delta_n)^{1/2}$$

and

$$k_{\rm I}=\kappa_\nu k_{\rm II}\ ,$$

where

$$\kappa_\nu=\left[\frac{2}{\nu+\frac{1}{2}}\right]^{1/2}\frac{\Gamma(1+\nu/2)}{\Gamma(\frac{1}{2}+\nu/2)} \tag{A9}$$

and we have also made use of the parametrization (2.23).

Finally, we shall briefly discuss the pole condition for the potential depicted in Fig. 5., namely two semiharmonic wells of different curvature $M\omega_{\rm I}^2$ and $M\omega_{\rm II}^2$, respectively. These wells are joined together at the origin, as shown in Fig. 5. For a trajectory of energy $E=\hbar\omega_{\rm I}(\nu+\frac{1}{2})=\hbar\omega_{\rm II}(\mu+\frac{1}{2})$, the reflection factors assume the form

$$r_{\rm I}=-r_{\rm II}=\frac{\kappa_\nu-\kappa_\mu}{\kappa_\nu+\kappa_\mu} \tag{A10}$$

where κ_ν is given by (A9). The pole condition for this potential is given by

$$1-t_{\rm I}\frac{r_M F_{\rm I}}{(1-r_{\rm I}r_M F_{\rm I})}\frac{r_M F_{\rm II}}{(1-r_{\rm II}r_M F_{\rm II})}t_{\rm II}=0\ , \tag{A11}$$

in which $F_{\rm I}$ and $F_{\rm II}$ are the contributions from the half cycle in each part of the Minkowskian regions, i.e., $F_{\rm I}=\exp[i\pi(\nu+\frac{1}{2})]$ and $F_{\rm II}=\exp[i\pi(\mu+\frac{1}{2})]$. The eigenvalue spectrum obtained from (A11) is exactly identical to that obtained by smoothly matching the parabolic cylinder functions[17] $D_\nu(y_{\rm I})$ and $D_\mu(y_{\rm II})$ where $y_i=(2M\omega_i/\hbar)^{1/2}q$, $i={\rm I,II}$. As the energy is increased both κ_μ and κ_ν approach unity. Thus, the reflection factors $r_{\rm I}$ and $r_{\rm II}$ approach zero. Consequently, for the highly excited states, one obtains the eigenvalue condition

$$1+F_{\rm I}F_{\rm II}=0 \tag{A12}$$

as can be expected from naive considerations.

*Present address: Lehrstuhl für Theoretische Physik, Universität Augsburg, Memminger Str. 6, D-8900 Augsburg, West Germany.

†Permanent address: Institute for Theoretical Physics, University of Stuttgart, Pfaffenwaldring 57, D-7000 Stuttgart-80, West Germany.

[1]P. Hanggi, J. Stat. Phys. **42**, 105 (1986).

[2]G. Gamow, Z. Phys. **51**, 204 (1928).

[3]E. U. Condon and R. W. Gurney, Nature (London) **122**, 439 (1928).

[4]M. von Laue, Z. Phys. **52**, 726 (1928).

[5]For example, see M. A. Preston and R. K. Bhaduri, *Structure of the Nucleus* (Addison-Wesley, Reading, Mass. 1975), Chap. 11.

[6]R. P. Feynman and A. R. Hibbs, *Quantum Mechanics and Path Integrals* (McGraw-Hill, New York, 1965); R. P. Feynman, *Statistical Mechanics* (Benjamin, New York, 1972).

[7](a) A. M. Polyakov, Phys. Lett. **59B**, 82 (1975); (b) I. Affleck and F. DeLuccia, Phys. Rev. D **20**, 3168 (1979).

[8]S. Coleman, in *The Whys of Subnuclear Physics*, edited by A. Zichichi (Plenum, New York, 1979), pp. 805–916; Phys. Rev. D **15**, 2929 (1977); C. G. Callan and S. Coleman, *ibid.* **16**, 1762 (1977).

[9]A. Patrascioiu, Phys. Rev. D **24**, 496 (1981).

[10]R. F. Dashen, B. Hasslacher, and A. Neveu, Phys. Rev. D **10**, 4114 (1974).

[11]U. Weiss and W. Haeffner, Phys. Rev. D **27**, 2916 (1983).

[12](a) S. Levit, J. W. Negele, and Z. Paltiel, Phys. Rev. C **22**,

1979 (1980); (b) B. R. Holstein and A. R. Swift, Am. J. Phys. **50**, 833 (1982); (c) A. Auerbach, S. Kivelson, and D. Nicole, Phys. Rev. Lett. **53**, 411 (1984); **53**, 2275(E) (1984).

[13]M. C. Gutzwiller, J. Math. Phys. **12**, 343 (1971); **11**, 1791 (1970); **10**, 1004 (1969); **8**, 1979 (1967).

[14](a) W. H. Miller, Adv. Chem. Phys. **25**, 69 (1974); J. Chem. Phys. **62**, 1899 (1975); W. H. Miller and T. F. George, J. Chem. Phys. **56**, 5637 (1971); (b) P. Pechukas, Phys. Rev. **181**, 166 (1969); **181**, 174 (1969); (c) K. F. Freed, J. Chem. Phys. **56**, 692 (1971).

[15]A. O. Caldeira and A. J. Leggett, Ann. Phys. (N.Y.) **149**, 373 (1983); **153**, 445(E) (1984); H. Grabert, U. Weiss, and P. Hanggi, Phys. Rev. Lett. **52**, 2193 (1984); U. Weiss and H. Grabert, Phys. Lett. **108A**, 63 (1985); P. Riseborough, P. Hanggi, and E. Freidkin, Phys. Rev. A **32**, 489 (1985); A. I. Larkin and Yu. N. Ovchinnikov, Zh. Eksp. Teor. Fiz. **86**, 719 (1984) [Sov. Phys.—JETP **59**, 420 (1984)]; S. Chakravarty and A. J. Leggett, Phys. Rev. Lett. **52**, 5 (1984); H. Grabert and U. Weiss, *ibid.* **54**, 1605 (1985).

[16]S. Washburn, R. A. Webb, R. F. Voss, and S. M. Faris, Phys. Rev. Lett. **54**, 2712 (1985); D. B. Schwartz, B. Sen, C. N. Archie, A. K. Jain, and J. E. Lukens, *ibid.* **55**, 1547 (1985); J. M. Martinis, M. H. Devoret, and J. Clarke, *ibid.* **55**, 1543 (1985).

[17]*Handbook of Mathematical Functions,* edited by M. Abramowitz and I. A. Stegun (Dover, New York, 1986), p. 687, 7th printing.

[18]L. S. Schulman, *Techniques and Applications of Path Integration* (Wiley, New York, 1981), Chap. 17.